

AFRL-SR-AR-TR-03-

0409

Standard Form 298 (Rev. 8-98)
Prescribed by ANSI Std. Z39.18

20031028 198

Objectives

Microspacecraft are currently considered by Air Force, NASA and industry for a variety of applications. Characteristics of a microspacecraft include dimensions less than 10 cm, weight less than 1 kg, and power below 10 W. These requirements clearly necessitate the need for microtechnologies and among them a critical one is micropropulsion. The mathematical and computational work investigated new issues that arise in simulating gas and plasma microthrusters that are an order of magnitude smaller than the existing state-of-the art. Flows in these microthrusters exhibit distinct physical characteristics that make computational modeling challenging. Current simulation technologies are based on continuum mathematical models and assumptions that break down in microscales and, therefore, cannot treat these microflows comprehensively. In addition, unlike the classical aerodynamic flows that are governed by predominantly hyperbolic behavior, flows in microthrusters are strongly viscous and, thus, exhibit parabolic behavior. Plasma microthrusters introduce an additional complexity in their analysis due to the overlap of electrodynamic and gasdynamic scales.

This research aimed overall at a unified mathematical formulation and numerical discretization of multi-species, partially ionized plasma micro-flows in non-equilibrium and involved closed interaction between two research groups. The group lead by Prof. Gatsonis at WPI developed a seamless Particle-In-Cell/Monte Carlo methodology and the group lead by Prof. Karniadakis at Brown University developed a semi-continuous spectral/hp methodology based on the multi-species, compressible, viscous-MHD equations. The developed methodologies were applied to the modeling of the micro-Pulsed Plasma Thruster, other micropropulsion thrusters, and related devices.

The major accomplishments are outlined below:

- Developed an adaptive unstructured grid generator with an enhanced optimization capability (Kovalev, 2000; Hammel, 2002)
- Developed an efficient particle-transfer algorithm during grid adaptation.
- Implemented neutral and charged particle transport algorithms on unstructured grids.
- Implemented elastic neutral-neutral, elastic ion-neutral and charge exchange ion-neutral collisions via the no-time-counter method.
- Implemented the Larsen-Borgnakke model for energy redistribution for rotational and vibrational degrees of freedom.
- Implemented a finite-volume method for Poisson's equation that utilized the Voronoi-Delauney mesh and implemented a GMRES solver to the discrete Poisson equation.
- Performed simulations of non-ionized flows in micronozzles as well as MEMS-based micronozzles (Hammel et al., 2001, Hammel, 2002).
- Performed simulations of plasma flows in electric micropropulsion devices such as the micro Field Emission Array (Gatsonis and Spirkin, 2002) and the micro Retarding Potential Analyzer (Spirkin and Gatsonis, 2003).
- Investigated high-order particle/force weighting and evaluated of fluctuations in the unstructured simulation of collisionless, fully- ionized plasmas (Spirkin and Gatsonis, 2003).
- Assisted Brown University in the development of an ablation model for micro-PPT simulations. Simulations also are underway that couple the continuous results from the multi-fluid code (Brown University) with the DSMC/PIC plume simulations.

Accomplishments/New Findings

1. Unstructured 3D PIC/DSMC Methodology

1.1 Grid Generation and Adaptation

An unstructured grid generator has been developed that provides three-dimensional meshes for arbitrary geometric configurations and adapts existing meshes according to the preliminary solution obtained on an initial grid (Kovalev, 2000; Hammel, 2002). The unstructured mesh generator is based on Watson's

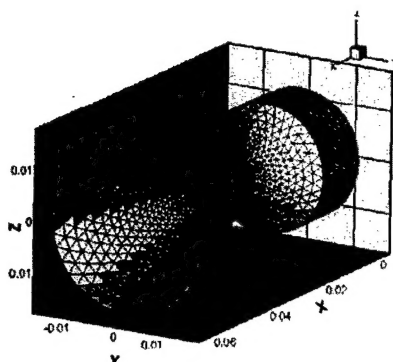


Figure 1. Surface discretization of a micronozzle.

in length gradually between the h -values of the edge vertices. The prospective nodes are filtered in order to satisfy the spacing and grid quality criteria. Nodes falling too close to existing nodes are eliminated. Nodes that worsen grid quality as specified by the lowest dihedral angle in a set of cells are also discarded. The nodes that are not rejected are inserted into the grid via Watson's algorithm. The edge

(1981) incremental node insertion method, which uses properties of the Delaunay triangulation. An initial mesh is required for Watson's method, in order to have a domain where point insertion to begin. The initial mesh chosen is a cube divided into six tetrahedra. After the initial mesh is generated, the source geometry is inserted into the domain. The underlying sizing function – defined by the source geometry – requires the interior of the grid to be enriched with nodes to the specified density. For this purpose the algorithm by Borouchaki and George (1997) was implemented and extended to three dimensions. In this algorithm, the characteristic distance between nodes is specified for each grid node based on mean-free path or the Debye length. Every existing edge of the grid is divided into a number of new prospective nodes, so that the new resulting edge segments vary

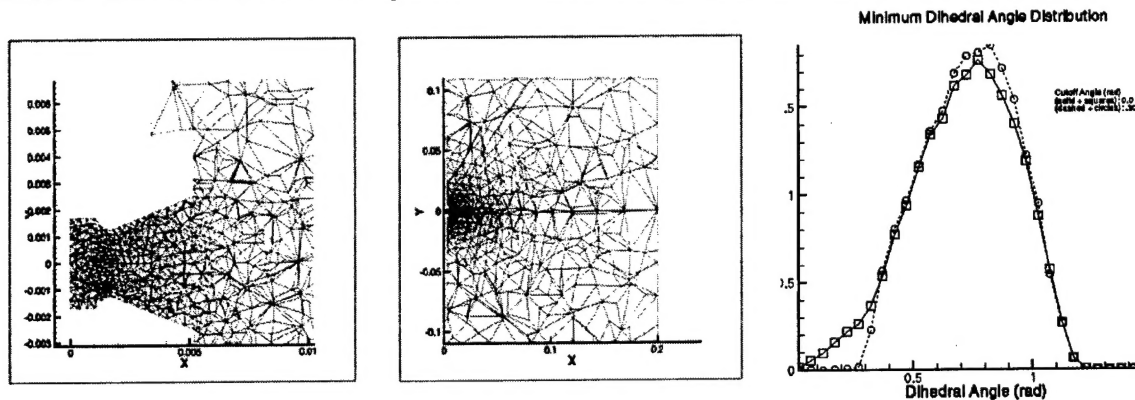


Figure 2. Cross-section of grid used in the simulation of a plenum/nozzle/plume flow of a microthruster. (Left) Details of the plenum/nozzle grid (Center) Overall simulation area (Right) Dihedral angle distribution based on the heuristic optimization criterion. (Hammel et al., 2001)

division process is repeated while new nodes are inserted. An example of the surface discretization is shown in Figure 1 and of the grid-generator in Figure 2. A heuristic quality improvement procedure has been also implemented based on a user-defined minimum dihedral angle. Figure 2 shows the improved distribution of dihedral angles with the application of optimization.

Adaptation is necessary for quality PIC, DSMC or PIC/DSMC computations in absence of a priori knowledge of the flow because the cell size must be of the order of the Debye length or the mean free path, which is an unknown local flow characteristic. Also, regions in which high gradients of flow variables occur have to be refined in order to provide a quality solution, and regions with very small gradients are coarsened to save computational time. The developed grid generator and the flow solver interact with each other, so that the adaptation is performed automatically after the initial solution is obtained. In addition we developed algorithms for the fast-transfer of data between adaptation.

1.2 Particle Loading, Injection and Motion

The general procedures for loading and injection used in this work follows Birdsall and Langdon (1991) and Bird (1994). The equation that describes the position of a neutral particle is updated from the post-collision velocity according to

$$\frac{d\mathbf{r}}{dt} = \mathbf{v} \quad (1)$$

The equations that describe the motion of a charged particle are

$$\frac{d\mathbf{r}}{dt} = \mathbf{v}, \quad \frac{d\mathbf{v}}{dt} = \frac{q}{m}(\mathbf{E} + \mathbf{v} \times \mathbf{B}) \quad (2)$$

Integration is based on a leapfrog scheme following a method developed by Boris, (1970). Particles are

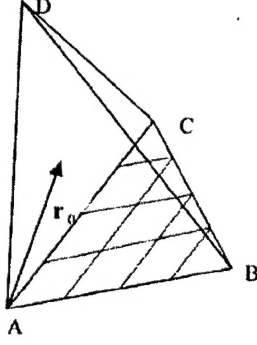


Figure 3. Tetrahedral cell.

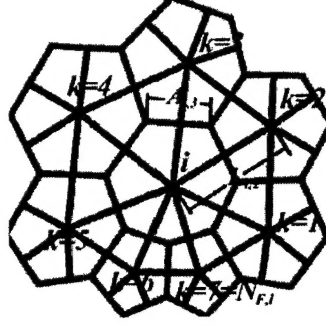


Figure 4. Delaunay-Voronoi mesh in 2D.

moved between adjacent tetrahedral cells using a particle-tracing technique. Following Figure 3, the intersection of a particle with initial position \mathbf{r}_0 and velocity \mathbf{v} with face ABC is

$$\mathbf{r}_0 + \mathbf{v}\tau = \alpha\overline{AB} + \beta\overline{AC} \quad (3)$$

where, τ is the time elapsed in moving from the initial point to the plane defined by points A, B, and C; α and β define the point of intersection in the skewed coordinate system of face ABC. If the time τ is negative, an intersection does not occur. If α or β are less than zero or

greater than unity, an intersection does not occur within the face. If the sum of α and β is greater than unity, then the intersection occurs outside the face. Particle-tracking algorithms are particularly slow in unstructured grids and fast particle-search algorithms are currently under investigation.

1.3 Collision Methodology

The particle motion and collisions are decoupled in our implementation, following the standard DSMC procedure. Elastic collisions are based on the no time counter (NTC) methodology (Bird, 1994) with molecular cross-section given by the variable hard sphere (VHS) model. Simulation of energy transfer to and from rotational degrees of freedom is based on the phenomenological model of Larsen-Borgnakke. Vibrational degrees of freedom are modeled as discrete, evenly spaced energy levels using the harmonic oscillator model. Vibrational energy redistribution is performed prior to rotational energy redistribution in the collision process, following Bird. If vibrational energies become high enough, the spacing between levels lessens and an anharmonic model must be used which may include dissociation as outlined by Bird (Hammel, 2002).

1.4 Poisson's Equation Solver

Solution of Poisson's equation

$$\nabla^2\Phi = -\sum_{i=1}^{N_i} q_i n_i + q_e n_e / \epsilon_0 \quad (4)$$

is based on a finite volume formulation that takes advantage of the Voronoi dual of the Delaunay triangulation. The Voronoi cell corresponding to each Delaunay node contains the set of points closer to the point than any other, the facets of the Voronoi cell are orthogonal to the lines joining the tetrahedral nodes as shown in Figure 4. For a node-centered finite-volume scheme with finite volume i associated with node i with a number of faces N_F the semi-discrete equation form of Gauss's law is

$$\sum_{k=1}^{N_F} \nabla\Phi \cdot (\hat{\mathbf{n}} A)_{i,k} = \sum_{k=1}^{N_F} \left(A \frac{\partial\Phi}{\partial n} \right)_{i,k} = -\frac{Q_i}{\epsilon_0} \quad (5)$$

In the above, Q_i is the total charge enclosed by volume i , $A_{i,k}$ is the area of the face k of associated with volume i , and the summation is over all the faces of the finite volume as shown in Figure 4 for a 2-D case.

Also, $A_{i,k}=(A \hat{n})_{i,k}$ is the magnitude of the area of the face k for the volume associated with node i multiplied by the unit outward normal vector. An approximation of the electric flux into a cell containing node i across a Voronoi face corresponding to an edge with nodes k and i is:

$$\sum_{k=1}^{N_{F,i}} \nabla \Phi \cdot (\hat{n} A)_{i,k} = \frac{A_{i,k}}{L_{i,k}} (\Phi_k - \Phi_i) \quad (6)$$

In the above, $L_{i,k}$ is the distance from node i to node k . Summing over all faces k of a Voronoi cell corresponding to node i , a system of linear equations may be formed assuming the charge inside the volume, Q_i , is known. The method reduces to the standard 2nd order finite-difference method on Cartesian meshes. The matrix form of this equation is:

$$\begin{bmatrix} R_{1,1} & R_{1,2} & R_{1,3} & \cdots & R_{1,N} \\ R_{2,1} & R_{2,2} & R_{2,3} & \cdots & R_{2,N} \\ R_{3,1} & R_{3,2} & R_{3,3} & \cdots & R_{3,N} \\ \vdots & \vdots & \vdots & \ddots & \vdots \\ R_{N,1} & R_{N,2} & R_{N,3} & \cdots & R_{N,N} \end{bmatrix} \begin{bmatrix} \Phi_1 \\ \Phi_2 \\ \Phi_3 \\ \vdots \\ \Phi_N \end{bmatrix} = \frac{1}{\epsilon_0} \begin{bmatrix} Q_1 \\ Q_2 \\ Q_3 \\ \vdots \\ Q_N \end{bmatrix} \quad (7)$$

N is the number of nodes in the mesh. The coefficients are determined by

$$R_{i,j} = \sum_{k=1}^{N_{F,i}} \frac{A_{i,k}}{L_{i,k}} \text{ for } i=j, \quad R_{i,j} = -\frac{A_{i,j}}{L_{i,j}} \text{ if } j \text{ is adjacent to } i, \quad R_{i,j} = 0 \text{ otherwise.}$$

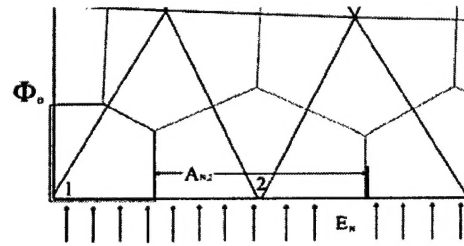


Figure 5. Boundary nodes.

$\frac{A_{i,j}}{L_{i,j}}$ is the ratio of the area of the Voronoi face between nodes i and j to the distance between nodes i and j if the nodes. The system of equations is solved using GMRES.

In a bounded domain, a solution of the Poisson's equation is specified by piece-wise Dirichlet and Neumann boundary conditions. For the boundary shown on the Figure 5, Node 1 is a Dirichlet boundary with potential Φ_0 , Node 2 is a node on a Neumann boundary with inward flux $E_{N,2}A_{N,2}$. Since the boundaries of the

Delaunay mesh are forced to coincide with the boundaries of the mesh, the implementation of boundary conditions is straightforward. In the case of Dirichlet boundary condition the voltage is placed on the right side hand of the matrix and the corresponding row zeroed with a one placed on the diagonal. Fluxes in the Neumann boundary conditions are added to the flux formulation for the Voronoi cell corresponding to the boundary node, the value of the inward normal electric field multiplied by the boundary area is added to the right hand side of the node of interest.

1.5 Particle and Force Weighting/Interpolation

Two weighting calculations are the part of a PIC timestep loop: accumulation of charge at grid nodes (weighting) and distribution of electric field to particle position (interpolation). Numerically these interpolations are implemented in terms of cloud shape function S or assignment function W as in Hockney and Eastwood (1999) or just in terms of assignment function W , which is referred to as weighting function (Birdsall and Langdon, 1991). Assignment functions of zero (NGP) and first order (Lagrange polynomials) are used in our PIC/DSMC code. Implementation of higher order schemes can improve the quality of PIC simulations. However, construction of such schemes on 3-D unstructured grids leads to complex analytical formulations that increase the computational time drastically. In order to eliminate the self-force and conserve momentum the 'momentum conservation' implementation is pursued where the weighting and interpolation function are identical.

1.6 Numerical Heating

An important quantity in plasma simulations, is the degree of numerical heating associated with a non-physical increase in the total energy of the system. The numerical heating is described in terms of the

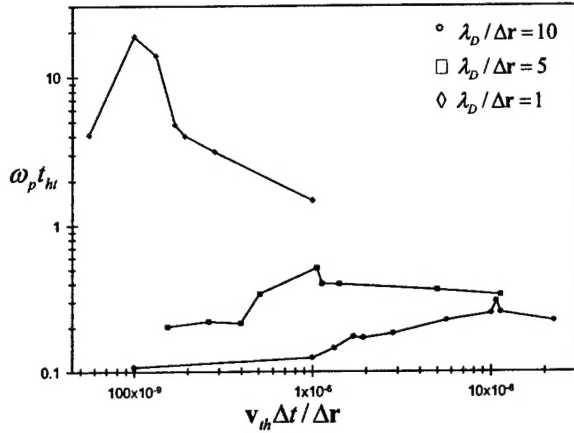


Figure 6. Heating time as a function of Δt and Δr for NGP assignment scheme.

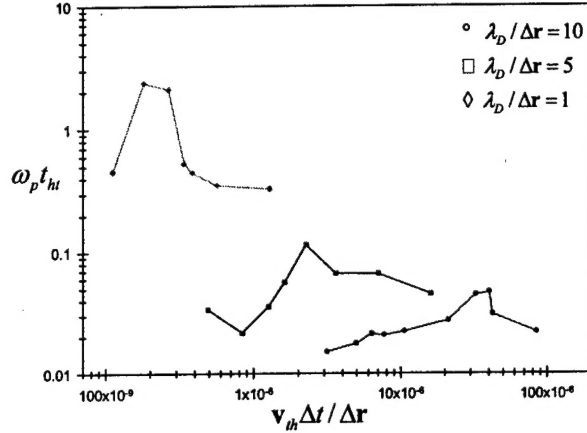


Figure 7. Heating time as a function of Δt and Δr for Linear assignment scheme

heating time τ_H , which measures the lack of energy conservation in the computational model and is infinite in real plasmas. In our analysis of the heating time we use the definition introduced by Hockney (1971) as the time that takes the energy of system to double. Results of the heating time calculations in Figures 6-7 show that for a specified $\lambda_D / \Delta r$, the timestep should be chosen from the specific range of values to produce the minimum numerical error. From Figures 6 and 7 it is evident that the heating time obtained when using linear weighting is about 10 times larger than the one for the NGP weighting. The energy-conserving implementation was also used to calculate τ_H , but it did not provide any advantage over the momentum-conserving scheme. (Spirkin and Gatsonis, 2003)

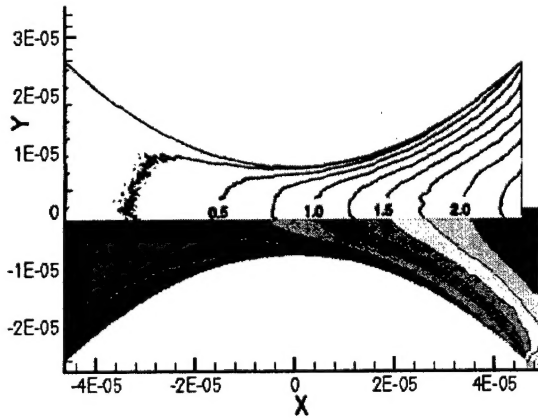


Figure 8. Mach numbers in a parabolic 15.4-micron micronozzle. Solid lines are from 2D DSMC simulations of Piekos and Breuer (1996).

2. Gaseous Micropropulsion Applications - DSMC

The unstructured DSMC modules of the code were validated with simulation of gaseous micronozzles and comparisons with previous experimental and numerical results (Hammel et al, 2001). Rothe's 5-mm diameter micronozzle operating at 80 Pa was simulated and results compared favorably with the experiments. The code was also applied to the simulation of a parabolic planar micronozzle with a 15.4-micron throat. Results shown in Figure 8 were compared favorably with previous 2D Monte Carlo simulations. The Gravity Probe-B micronozzle was simulated in a domain that includes the injection chamber and plume region. Stagnation conditions included a pressure of 7 Pa and mass flow rate of 0.012 mg/s. The simulation shown in

Figure 9, examined the role of injection conditions in micronozzle simulations and results are compared with previous Monte Carlo simulations. Finally, the code was applied to the simulation of a 34-micron

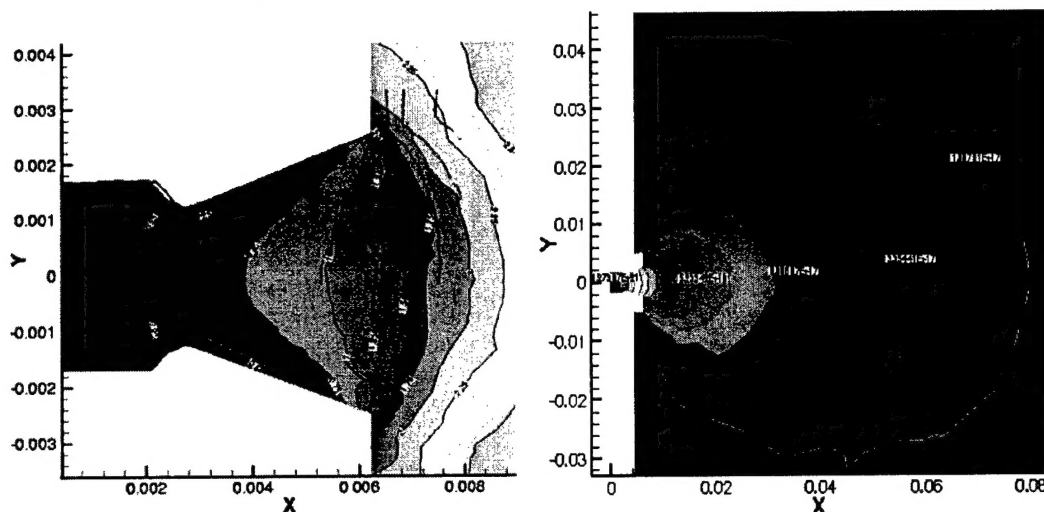


Figure 9. 3D Unstructured DSMC simulation of a combined plenum/nozzle/plume flow of a cold-gas microthruster. (Left)Mach numbers (Right) Number density in the plume region (Hamell et al., 2001).

throat MEMS fabricated micronozzle. This micronozzle is planar in profile with sidewalls binding the upper and lower surfaces. The stagnation pressure was set at 3.447 kPa and represents an order of magnitude lower pressure than used in previous experiments. The simulation demonstrated the formation of large viscous boundary layers in the sidewalls. (Hammel, 2002)

3. Electric Micropropulsion Applications -PIC

In Gatsonis and Spirkin (2002) we presented the PIC implementation of our PIC/DSMC code and simulations of field emission array (FEA) cathodes that can be an integral part of micropropulsion devices (Marrese et al., 2000a). Electron emission in a background plasma leads under certain conditions in the formation of a virtual-cathode that could limit the operation of such devices. Our simulations expanded

the work of Marrese et al. (2000b) by including emission with cold (0.1 eV) and hot (5 eV) electrons into a background 5-eV plasma. The emitted electron beam/background plasma coupling processes considered in our work are important not only in the operation of FEA cathodes but also in plume expansion as they elucidate basic plasma physics phenomena. Results in Figure 10 show the formation of virtual cathode under certain emission conditions. The simulations served also as means of validation of the newly developed PIC-modules of our PIC/DSMC code.

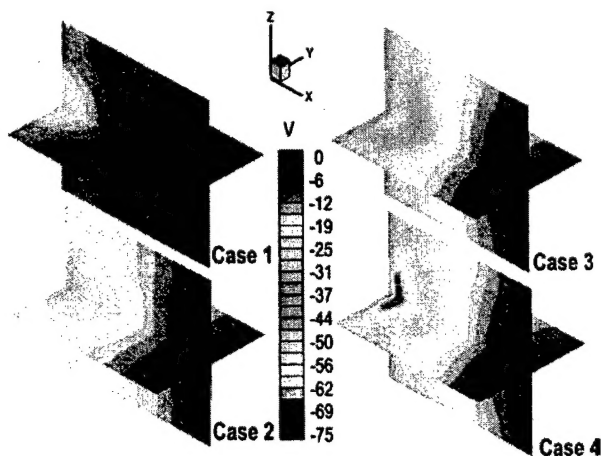


Figure 10. Potential in front of a field emission array from unstructured 3D PIC simulations (Gatsonis and Spirkin, 2002)

In Spirkin and Gatsonis (2003) the unstructured PIC code was used to simulate a directional-RPA currently under design by the PI to operate in a high-density plasma environment (Partridge et al., 2003). The simulations offered insights on the plasma flow inside the device and

are assisting the design process. The 3D simulations results showed the potential distribution in the segmented, micron-scale channel as well as the ion and electron flow characteristics. In an effort to

simulate the operation of the sensor, the current on the plate was evaluated and plotted as a function of the ion retarding potential. The simulations presented the energy distribution of the collected ions.

In Wheelock et al. (2003) the unstructured PIC code was implemented in the simulation of ion beam neutralization phenomena. This work is part of collaborative effort between the PI and Dr. Cooke of AFRL/VSBX, (Hanscom AFB). These simulations show the dependence of the beam neutralization on beam energy and neutralization current. The simulations served also as means of validation of the PIC-modules of our PIC/DSMC code by comparisons with 2D PIC simulations.

4. Development of Teflon Ablation Model

This effort was in collaboration between the PI and Professor Karniadakis (Brown University) and led in the development of an ablation model that is used in the continuum simulation of PPTs. The team included Visiting International Scholar Prof. Shurzhikov who was hosted by WPI and Brown University during the Summer of 2001.

5. Axisymmetric Hybrid Code

An associated effort involved a hybrid (particle-fluid) code that was developed by the PI with partial support from NASA Glenn Research Center (Gatsonis and Yin, 1999). The approach treats ions and neutrals as particles and electrons as fluid. We also implemented a new conservative method for weighting in axisymmetric coordinates. Added the full energy equation for electrons that include convective, conductive and collisional terms. Simulations of pulsed plasma plumes were compared with our triple and quadruple Langmuir probe data take in plumes of pulsed plasma thrusters. These hybrid methodologies validated in axisymmetric coordinates will be transferred to the 3D Unstructured DSMC/PIC code.

References

1. Bird, G.A., *Molecular Gas Dynamics and the Direct Simulation of Gas Flows*, Clarendon Press, Oxford, 1994.
2. Birdsall, C.K., A. B. Langdon, "Plasma Physics via Computer Simulations", *Plasma Physics Series*, 1991.
3. Boris, J.P., "Relativistic Plasma Simulation-Optimization of a Hybrid Code", Proceedings of the Fourth Conference on Numerical Simulation of Plasma, Naval Res. Lab, Washington D.C., 3-67, 2-3 November, 1970.
4. Borouchaki, H., George, P. L., "Aspects of 2-D Delaunay Mesh Generation," *International Journal for Numerical Methods In Engineering*, Wiley, Vol. 40, pp.1957-1975, 1997
5. Gatsonis, N.A., Spirkin, A., "Unstructured 3D PIC Simulations of Field Emission Array Cathodes for Micropropulsion Applications," AIAA 2002-3687, 38th AIAA/ASME/SAE/ASEE Joint Propulsion Conference, Indianapolis, Indiana, July 2002
6. Hammel, J., Kovalev, K., Gatsonis, N.A., "Unstructured Adaptive Monte Carlo Simulations of Flows in Micronozzles," AIAA 2001-2891, 35th AIAA Thermophysics Conference, Anaheim, CA, June, 2001
7. Hockney, R.W., "Measurements of Collision and Heating Times in a Two-Dimensional Thermal Computer Plasma", *Journal Of Computational Physics* 8, 19-44, 1971.
8. Hammel, J., "Development of an Unstructured 3-D Direct Simulation Monte Carlo/Particle-In-Cell Code and Simulation of Microthruster Flows," M.S. Thesis, WPI, Worcester, MA, March 2002.
9. Hockney, R.W., Eastwood, J.W., *Computer simulation using particles*, Adam Hilger, New York, 1988.
10. Kovalev, K., "Development of a 2D/3D Unstructured Adaptive Grid Generator for Direct Simulation Monte Carlo Computations," M.S. Thesis, WPI, Worcester, MA, July 2000.
11. Marrese C., Wang J. et al. "Field Emission Cathodes in Xenon EP Systems", *Progress in Astronautics and Aeronautics Vol. 187: Micropropulsion for Small Spacecraft*, AIAA, ed. Micci and Ketsdever, 2000a

12. Marrese C., Wang J. et al. "Space-Charge-Limited Emission from Field Emission Cathodes for Electric Propulsion and Tether Applications", *Progress in Astronautics and Aeronautics Vol. 187: Micropropulsion for Small Spacecraft*, AIAA, ed. Micci and Ketsdever, 2000b.
13. Partridge, J., Gatsonis, N.A., Pencil, E., "Preliminary Design and Analysis of a Directional Micro-Retarding Potential Analyzer for High-Density Plumes", AIAA 2003-5172, 39th AIAA/ASME/SAE/ASEE Joint Propulsion Conference, Huntsville, AL, July 2003.
14. Piekos, E. S., Breuer, K. S., "Numerical Modeling of Micromechanical Devices Using the Direct Simulation Monte Carlo Method," *Journal of Fluids Engineering*, Vol. 118, September, 1996
15. Spirkin A., Gatsonis, "Unstructured 3D PIC Simulation of Plasma Flow in a Segmented Microchannel," AIAA 2003-3896, 36th AIAA Thermophysics Conference, Orlando, FL, June 2003.
16. Watson, D. F., "Computing the Delaunay Tessellation with Application to Voronoi Prototypes," *The Computer Journal*, Vol. 24(2), pp. 167-172, 1981
17. Wheelock, A., Cooke, D., Gatsonis, N.A., "Ion Beam Neutralization Processes For Electric Micropropulsion Applications" AIAA 2003-5148, 39th AIAA/ASME/SAE/ASEE Joint Propulsion Conference, Huntsville, AL, July 2003.

Personnel Supported

1. Dr. N. A. Gatsonis, (PI) Associate Professor of Mechanical Engineering (supported)
2. Dr. Sergey Surzhikov, International Visiting Scholar (supported, collaborative with Brown University)
3. Konstantin Kovalev, Graduate Research Assistant (supported)
4. Jeff Hammel, Graduate Research Assistant (supported)
5. Ph.D. Candidate, Anton Spirkin, Graduate Research Assistant (supported)
6. Ph.D. Candidate, Adrian Wheelock, Air Force Space Scholar (associated with the effort)
7. Andrew Suryali, Graduate Research Assistant (associated with the effort)

Publications

1. Spirkin A., Gatsonis, N.A., "Unstructured 3D PIC Simulation of Plasma Flow in a Segmented Microchannel," AIAA 2003-3896, June 2003.
2. Wheelock, A., Cooke, D., Gatsonis, N.A., "Ion Beam Neutralization Processes For Electric Micropropulsion Applications" AIAA 2003-5148, July 2003.
3. Gatsonis, N.A., Spirkin, A., "Unstructured 3D PIC Simulations of Field Emission Array Cathodes for Micropropulsion Applications," AIAA 2002-3687, July 2002.
4. Hammel, J., "Development of an Unstructured 3-D Direct Simulation Monte Carlo/Particle-In-Cell Code and Simulation of Microthruster Flows," M.S. Thesis, WPI, Worcester, MA, March 2002.
5. Hammel, J., Kovalev, K., Gatsonis, N.A., "Unstructured Adaptive Monte Carlo Simulations of Flows in Micronozzles," AIAA 2001-2891, CA, June, 2001.
6. Kovalev, K., "Development of a 2D/3D Unstructured Adaptive Grid Generator for Direct Simulation Monte Carlo Computations," M.S. Thesis, WPI, Worcester, MA, July 2000.

Interactions/Transitions

- a) Participation/Presentations of the AFOSR supported work at AFRL:
 1. Gatsonis N. A and Wheelock, A., "Advanced Particle and Particle/Fluid Simulations of Gaseous and Plasma Thruster/Plume Spacecraft Interactions: Towards an End-to-End Simulation Capability," Thruster Spacecraft Interactions Simulation Workshop, Air Force Research Lab, Edwards, CA, February 28, 2003.
 2. Gatsonis, N.A., "Coupling Continuum (Fluid) and Kinetic(Particle) Methods for the Simulation of Gaseous and Plasma Flows in Transition", Air Force Research Laboratory, Hanscom AFB, MA, January 23, 2003.

3. Gatsonis, N.A., "Recent Advances in Hybrid PIC", Air Force Research Laboratory Workshop on PIC-FDTD, Air Force Research Laboratory, Kirtland AFB, NM, August 22, 2001.
- b) Presentations of the AFOSR supported work:
1. Spirkin A., Gatsonis, N.A., "Unstructured 3D PIC Simulation of Plasma Flow in a Segmented Microchannel," AIAA 2003-3896, 36th AIAA Thermophysics Conference, Orlando, FL, June 2003.
 2. Wheelock, A., Cooke, D., Gatsonis, N.A., "Ion Beam Neutralization Processes For Electric Micropropulsion Applications" AIAA 2003-5148, 39th AIAA/ASME/SAE/ASEE Joint Propulsion Conference, Huntsville, AL, July 2003.
 4. Gatsonis, N.A., "Continuum/Atomistic (Hybrid) Simulations of Gaseous and Plasma Flows in Transition", Otto H. York Department of Chemical Engineering, NJIT, Newark, NJ, November 18, 2002.
 3. Gatsonis, N.A., Spirkin, A., "Unstructured 3D PIC Simulations of Field Emission Array Cathodes for Micropropulsion Applications," AIAA 2002-3687, 38th AIAA/ASME/SAE/ASEE Joint Propulsion Conference, Indianapolis, Indiana, July 2002.
 4. Gatsonis, N.A. and Hammel J., "Development of a DSMC/PIC Model for Flows in Plasma Microthrusters", 27th International Electric Propulsion Conference, Pasadena, CA, October 15, 2001.
 5. Gatsonis, N.A. and Suryali, A., "Effects of Plasma Background on PPT Plume Expansion", 27th International Electric Propulsion Conference, Pasadena, CA, October 15, 2001.
 6. Hammel, J., Kovalev, K., Gatsonis, N.A., "Unstructured Adaptive Monte Carlo Simulations of Flows in Micronozzles," AIAA 2001-2891, 35th AIAA Thermophysics Conference, Anaheim, CA, June, 2001.
 7. Gatsonis, N.A. and Hammel J., "A 3D Electrostatic DSMC/PIC Model on Unstructured Grids and Applications to Plasma Microflows", IEEE Pulsed Power Plasma Science Conference, Las Vegas, NV, June 18, 2001.

The PI has been also:

1. Chair, Session 83-EP-16 on Plumes and Spacecraft Interactions I, ASME/AIAA/SAE/ASEE 39th Joint Propulsion Conference, Huntsville, AL, July 22, 2003.
2. Chair, Session EP-18 on Electrothermal Thrusters, ASME/AIAA/SAE/ASEE 37th Joint Propulsion Conference, Salt Lake City, UT, July 11, 2001.
3. Chair, Session TP-18 on Microscale Flows, 35th AIAA Thermophysics Conference, Anaheim, CA, June 13, 2001.
4. Conference Organizer for 18 Electric Propulsion sessions, ASME/AIAA/SAE/ASEE 36th Joint Propulsion Conference, Huntsville, AL, July 16-19, 2000.

c) Transitions/Interactions

1. This research was pursued in interaction with Prof. G. Karniadakis of Brown University whose AFOSR-funded research pursued the development of a semi-continuous spectral/hp methodology for the compressible, viscous-MHD equations.
2. Results of this research assisted a PPT plume modeling and experimental effort supported by NASA Glenn Research Center (Technical Monitor, Eric Pencil, Eric.Pencil@grc.nasa.gov).
3. In Summer 2002 the PI began a collaboration with Dr. David Cooke (AFRL/VSBX, David.Cooke@hanscom.af.mil) on simulation and experiments of ion beam neutralization phenomena. This interaction included the WPI graduate student Adrian Wheelock who became an Air Force Space Scholar. Results of this collaboration were presented in Wheelock et al., 2003.